

---

## Machining of Fe17Cr2Ni0.2C iron based thermally sprayed coatings by turning with special interest to the influence of the depth of cut

H. Liborius<sup>1</sup>, A. Nestler<sup>1</sup>, G. Paczkowski<sup>2</sup>, A. Schubert<sup>1</sup>, T. Grund<sup>2</sup>, T. Lampke<sup>2</sup>

<sup>1</sup> Professorship Micromanufacturing Technology, Chemnitz University of Technology, Germany

<sup>2</sup> Professorship of Materials and Surface Engineering, Chemnitz University of Technology, Germany

*hendrik.liborius@mb.tu-chemnitz.de*

---

### Abstract

Additive manufacturing processes offer an enhancement of the diversity of geometry and the fields of application. Increasing demands on the complexity of modern components result in limitations concerning material selection or higher investments as a consequence of adapted production processes (machines, tools, process parameters). However, the material selection is restricted by the service conditions. The coating by thermal spraying represents an auspicious approach for a solution of this problem, by partly decoupling the properties of the substrate material and the surface. Thermally sprayed cylinder liners in combustion engine blocks consisting of aluminium alloys are a representative example. The additive manufactured coatings have to be machined to reach adequate properties of the tribological system (sprayed cylinder liner and piston with its piston rings). So far, finish machining is done by honing. A substitution of the machining with geometrically undefined cutting edges by finish boring would lead to a minor environmental impact. Furthermore, a shorter machining time and reduced production costs are aspired.

In the investigations specimens, exhibiting a helical surface dovetail microstructure, are coated by atmospheric plasma spraying (APS). For finish machining indexable inserts with CBN tips, a rake angle of 0° and sharp cutting edges are used. In the experimental investigations, with a constant cutting speed (250 m/min) and feed (0.05 mm) the depth of cut is varied between 0.01 mm and 0.2 mm. The components of the resultant force are measured while machining. Subsequently the tool wear is analysed microscopically. The geometrical properties of the surface are determined by tactile measurements and 3D laser scanning microscopy. The analyses include the detection of opened pores, pulled out coating material and oxides at the machined surface. Additionally residual stresses are analysed based on the results of XRD. An increase of the depth of cut results in increasing components of the resultant force and tool wear. The values for Ra, Rz, and Rvk decrease slightly. With increasing depth of cut the residual stresses decrease in the feed direction and increase in the cutting direction.

The results in turning of thermally sprayed iron based coatings contribute to the expansion of the application field of coatings produced by additive processes. Additionally, they contribute to the substitution of the honing of cylinder linings by machining with geometrically defined cutting edges. Summarised the results enable a more material and energy efficient production.

Turning; Thermally sprayed coatings; Surface integrity

---

### 1. Introduction

Increasing demands for passenger cars considering the emission of CO<sub>2</sub> and the raising scarcity of resources lead to changes in the selection of material. The use of lightweight materials such as aluminium alloys represent a possibility to engage with this problem. But these alloys often do not exhibit adequate surface properties, tribological properties, and chemical resistance. For this, the properties of the substrate and the surface have to be decoupled, which could be done by additive processes. In automotive industry for instance aluminium alloys are used as base material for combustion engine blocks. The cylinder linings are coated by iron based coatings, because aluminium alloys do not offer sufficient chemical resistance against modern fuels with their additives. Additionally, these coatings have microstructure inherent pores. While finish machining they are opened and act as lubricant reservoir in service, which results in enhanced tribological properties. Therefore honing is used for finish machining because the process enables to open the pores. A substitution

of this abrasive process by machining with geometrically defined cutting edges would result in a minor environmental impact and maybe a more economic manufacturing.

For finish machining and in service a high adhesive strength between substrate and coating is required. To ensure this, microstructuring of the substrate is necessary. This could be done by grit blasting, water jet cutting, laser machining, or process with geometrically defined cutting edges. Microstructuring by turning enables to produce a dovetail microstructure. Bobzin et al. [1] showed that these microstructures enhance the adhesive tensile strength compared to grit blasted substrates. Detailed experimental investigations of Hoffmeister et al. [2] showed a minimum dovetail microstructure height of 70 µm for interlocking between substrate and coating. With increasing height the adhesive tensile strength between substrate and coating raised. In the experimental investigation of Liborius et al. [3] the distance between the dovetail structure elements and subsequently the number of structure elements per length was varied. A higher number of structure elements per length resulted in an increased adhesive tensile strength at the

interface of the substrate and the coating. Additionally, the oxide proportion and the hardness of the coating increased with decreasing distance between the structure elements.

Ding et al. [4] analysed the influence of the cutting material in finish boring of iron based thermally sprayed coatings. Cermet tools, cemented carbide tools, diamond tipped tools and two different CBN tipped tools (50 % boron nitride bounded by a ceramic binder and 90 % boron nitride bounded by a metallic binder) were used. Regarding the tool wear the CBN tipped tools exhibited significant advantages in comparison to the other cutting materials tested.

In the experimental investigations of Liborius et al. [5] thermally sprayed iron based coatings were machined by turning. The cutting speed was varied in the range between 100 m/min and 400 m/min. Afterwards, the surfaces machined with cutting speeds between 200 m/min and 400 m/min exhibited similar geometrical properties. Additionally tool wear raised with increasing cutting speed because of increasing temperature in the shear zone and higher kinetic energy of the oxides.

Regarding the state of the art there are no investigations concerning the influence of the depth of cut on the properties of the surface and the surface layer in turning of iron based thermally sprayed coatings. Increasing the knowledge of the mechanisms in the cutting process represent a significant step for the substitution of the common honing process by finish machining with geometrically defined cutting edges.

## 2. Methodology

### 2.1. Substrate microstructuring

To generate an adequate adhesive tensile strength at the interface of the substrate and the coating the substrates were microstructured by a helical dovetail microstructure, shown in Fig. 1.

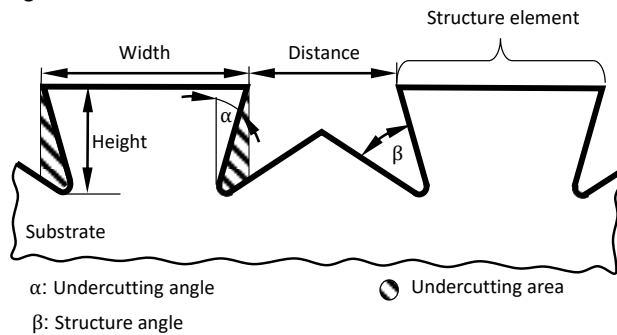


Figure 1. Dovetail substrate microstructure in cross section

The substrate microstructure was designed with a height of 70  $\mu\text{m}$ . In conjunction with the undercutting angle of 15° and the width of 93  $\mu\text{m}$  an undercutting area of about 1,230  $\mu\text{m}^2$  per structure element occurred. Regarding the distance of 240  $\mu\text{m}$  between the structure elements the microstructure consisted of 3 structure elements per millimetre. Hence, an undercutting area of about 3,700  $\mu\text{m}^2/\text{mm}$  was offered (determined at cross section in the feed direction).

For the experiments cylindrical specimens consisting of the aluminium alloy EN AW-5754 with a diameter of 50 mm and a length of 50 mm were used. The microstructuring of the substrates by turning as well as the finish machining experiments (2.3) were carried out on a SPINNER PD 32 precision lathe. For Microstructuring MCD tipped tools were used. The cutting edges were produced by grinding and polishing. The corner radius of 10  $\mu\text{m}$  was approximated by three facets with a length of about 6  $\mu\text{m}$ . The tools are characterised by a corner

angle of 50°, which represents the structure angle with the same value. The undercutting angle was determined by the tool cutting edge angle, which was kept constant with 105°.

Microstructuring was done in two consecutive steps similar to Liborius et al. [5]. For both steps the machining parameters were equal. The rotational speed was kept constant with 1,275  $\text{min}^{-1}$ , which correlates to a cutting speed of about 200 m/min. This enables an adequate cutting of the material and low tool wear. Additionally, an emulsion flood cooling was used to avoid built-up edge formation. The feed applied of 0.333 mm corresponded to the sum of the distance and the width of the structure elements. The height of 70  $\mu\text{m}$  of the structure elements was reached in 10 steps with a depth of cut of 7  $\mu\text{m}$ . Additionally, an adjustment in the feed direction was necessary to manufacture the undercut.

### 2.2. Coating process

For the processing of the functional top coating, an one-anode/one-cathode F6 atmospheric plasma spray (APS) system by GTV Verschleißschutz GmbH, Germany, was used. The coating parameters are listed in Table 1. An example of the coated substrate in cross section is given in Fig 2.

Table 1 Parameters of the APS process

Current (A)	600 A
Power (kW)	34.2
Plasma gas (slpm)	Ar: 70 / H: 5
Powder feeding gas (slpm)	Ar: 3
Line spacing of the robot (mm)	5
Coating distance (mm)	150
Coating angle (vs. cylinder axis)	75°
Robot speed (vs. cylinder axis) (m/s)	0.01
Cylinder surface rotation speed (m/s)	0.1

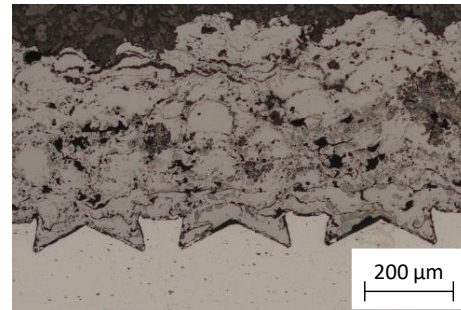


Figure 2. Coated substrate in cross section

### 2.3. Finish machining

After the APS process the specimens exhibited a roughness of more than 100  $\mu\text{m}$ . To ensure constant conditions for the machining experiments a pre-machining by several cutting steps with a depth of cut of 0.05 mm and a feed of 0.05 mm was done.

For the investigations the feed was kept constant with 0.05 mm, which enabled adequate surface properties in prior experiments regarding the influence of the feed. The cutting speed was chosen in accordance to previous experiments [5] with 250 m/min as a compromise of tool wear and surface properties and to reduce the effect of tool wear. The influence of the depth of cut (0.01 mm, 0.025 mm, 0.05 mm, 0.075 mm, 0.1 mm, 0.125 mm, 0.15 mm, 0.175, and 0.2 mm) was analysed. No lubrication was applied.

Indexable inserts of the type CCGW 09T304 (Sumitomo) with CBN tips were used for the turning experiments. The cutting material consisted of 90 % to 95 % boron nitride with a grain size of about 1  $\mu\text{m}$ , bounded with a cobalt based binder. The cutting edges had no chamfer, resulting in a rake angle of 0°. The tool

holder used led to a nominal tool cutting edge angle of 95°. Every tool was used for the machining of two specimens. To detect the components of the resultant force the tool holder was mounted on a three-axis force dynamometer Kistler, type 9257A, which was connected to a charge amplifier (Kistler 5070A).

The tool wear was detected by light microscopy using a Keyence VHX-100 3D microscope and by a 3D laser scanning microscopy Keyence, type VK-9700.

#### 2.4. Surface properties

The geometrical surface properties were detected by tactile and optical methods. The surface roughness of all specimens machined was measured in the feed direction using a stylus instrument Mahr type LD 120. The measuring length was 4 mm. The filtering of the profile was done in accordance to ISO 11562. For a validation of the roughness values, each specimen was measured at five different positions in the middle of the specimens. In addition, the samples were measured with a 3D laser scanning microscope Keyence type VK-9700. The size of the measured area was 2.0 mm (in the feed direction) × 0.5 mm (in the cutting direction). The objective of the optical measurements was to determine the volume of the pores and of the material pulled out of the surface. For this, the software MountainsMap was used. To determine the valley void volume as accurately as necessary, first a form filter (polynomial 2<sup>nd</sup> order) was applied. Afterwards, the periodic kinematic roughness profile was removed from the surface (using the tool “line orientation”). The Abbott curve of the resulting surface was characterised by a small core roughness. Following this, the tangent in this area had a small slope. Therefore, the lower material ratio (Smr2) was determined, which gave an approximated and reproducible value for the proportion of pores and pulled out material. The Smr2 was used as upper boundary for calculating the valley void volume (Vvv).

The residual stresses in the machined surface layer were determined by X-ray diffraction utilising the  $\sin^2\psi$  method (diffractometer D8 Discover, Bruker AXS). The measurements were done with a cobalt anode on the {211}/{112} lattice planes of martensite using Young’s modulus  $E_{\{211\}} = 220$  GPa and Poisson’s ratio  $\nu_{\{211\}} = 0.28$ . An area with a diameter of about 0.7 mm was irradiated.

### 3. Results and discussion

#### 3.1. Components of the resultant force

The components of the resultant force occur as a result of friction and deformation in the machining process. The influence of the depth of cut on the components of the resultant force is shown in Fig. 3.

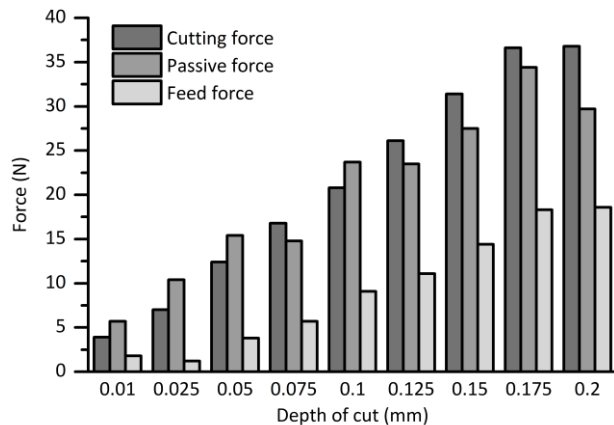


Figure 3. Influence of the depth of cut on the components of the resultant force

Increasing the depth of cut resulted in increasing components of the resultant force. This is explained by the raising cross section of undeformed chip. The feed force represented the lowest component of the result force with mean values between 1.2 N and 18.6 N. Cutting force and passive force were generally higher in the detected range of the depth of cut with mean values up to 34.4 N (passive force) and 36.6 N (cutting force). For lower depths of cut the passive force was higher compared to the cutting force. For increasing depths of cut this relation was changed and hence the cutting force was the dominant component of the resultant force.

#### 3.2. Tool wear

An example of the tool wear after machining with a depth of cut 0.1 mm is shown in Fig. 4.

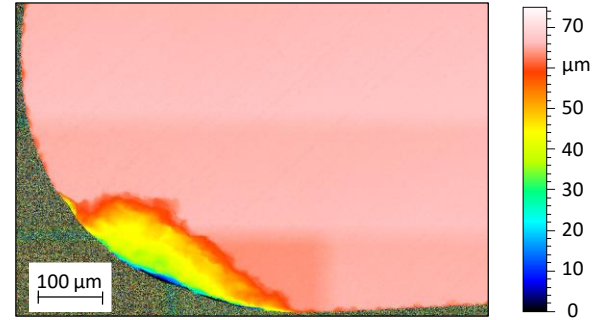


Figure 4. Tool wear detected by 3D laser scanning microscope after machining with a depth of cut of 0.1 mm

The tool wear after machining was qualitatively similar for all indexable inserts. Only the flank wear land width, which was measured particular to the rake between rake face and the deepest point at the cutting edge after machining changed. With increasing depth of cut the flank wear land width increased. For the lowest depth of cut a flank wear land width of 20  $\mu\text{m}$  was measured. For the highest depth of cut the detected flank wear land width was about 50  $\mu\text{m}$ . The increasing tool wear is a result of the increasing temperatures in the shear zone as a consequence of the higher cutting performance. Additionally, the tool rake angle was changed due the tool wear.

#### 3.3. Surface properties

Independent of the feed all specimens machined showed a kinematic roughness profile. Additionally, the surfaces were characterised by feed marks, cracks, pulled out coating material or oxides, and opened pores similar to previous results [5]. An example detected by 3D laser scanning microscopy after machining with the depth of cut of 0.1 mm is given in Fig. 5.

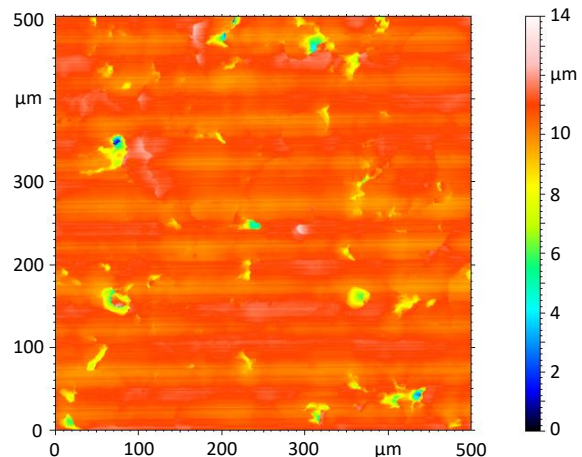


Figure 5. Surface detected by 3D laserscanning microscope after machining with a depth of cut of 0.1 mm

The influence of the depth of cut on Ra, Rz, and Rvk is shown in Fig. 6. The respective mean values represent the mean values out of five measurements at each specimen. The minimum and maximum are the respective highest and lowest values of these five measurements.

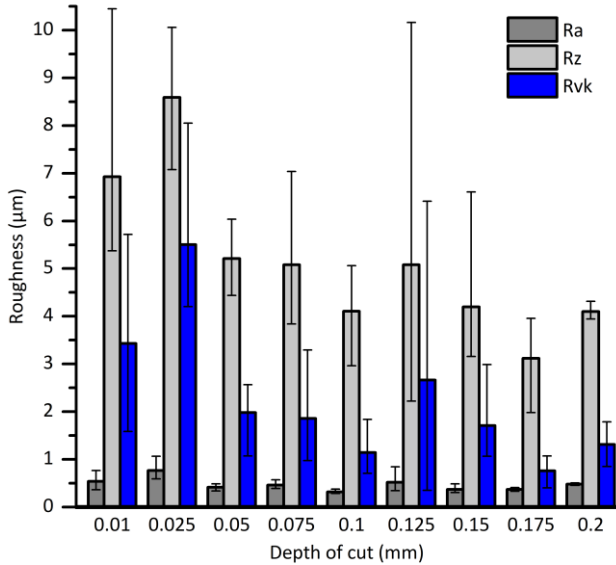


Figure 6. Influence of the depth of cut on Ra, Rz and Rvk

The mean values of Ra are nearly constant in the considered range of the depth of cut. Detailed analysis of the mean values show a slight decrease for higher depths of cut. The highest mean values were reached after machining with a depth of cut of 0.01 mm (Ra = 0.537 µm) and 0.025 mm (Ra = 0.766 µm). For increasing depths of cut the mean values were lower. The minimum was measured after machining with a depth of cut of 0.1 mm (Ra = 0.321 µm).

Regarding the mean values a tendency of decreasing of Rz and Rvk with increasing depth of cut is visible. The measured values for Rz were higher than the calculated kinematic roughness of 0.78 µm, which is a result of the cracks, pulled out coating material or oxides, and opened pores. The high variance of the values is also explained by these surface irregularities. The slight decrease of the mean values were a result of the increasing components of the resultant force. Especially the passive force, which was orientated particular the machined surface. As a consequence of the higher material deformation in the shear zone, less pores were opened and coating material or oxides were pulled out. This resulted in lower roughness values. The decreasing mean values occurred also due the increasing tool wear with higher depths of cut and therefore changing effective rake angle. The decrease of the rake angle led to less pulled out coating material and opened pores.

To enhance the determination of the proportion of opened pores and pulled out material Vvv was used. The influence of the depth of cut on Vvv for the first cut is shown in Fig. 7.

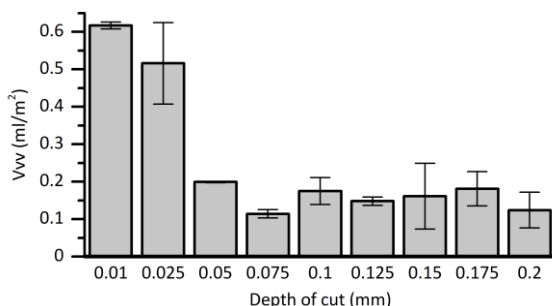


Figure 7. Influence of the depth of cut on Vvv

The maximum of Vvv was reached after machining with depths of cut of 0.01 mm and 0.025 mm. Increasing the depth of cut led to strongly decreased values of Vvv. Similar to Rvk this was explained by the increasing passive force, hence increasing stresses in this direction and therefore less pulled out coating material and opened pores.

### 3.4. Residual stresses

The influence of the depth of cut on the residual stresses is shown in Table 2.

Table 2 Influence of the depth of cut on the residual stresses in feed and cutting direction

Depth of cut (mm)	Residual stress (MPa) in	
	Feed direction	Cutting direction
0.01	-24	42
0.75	-33	55
0.125	-41	63
0.2	-49	106

An increase of the compressive residual stresses in the feed direction with increasing depth of cut was visible. This can be explained by the increasing proportion of plastic deformation as a result of the increasing components of the resultant force and thereby increasing stresses in the shear zone. In the cutting direction tensile residual stresses were measured. The amount also increased with increasing depth of cut, which was an effect of the increasing temperature as a consequence of the increasing cutting performance in the shear zone.

## 4. Summary and Conclusion

The results of the experimental investigations exhibit that the geometrically defined dovetail substrate microstructures enable an adequate adhesive tensile strength between the substrate and the coating for the finish machining by turning. Independent of the depth of cut, the specimens show a kinematic roughness profile with additional cracks, pulled out material and opened pores. In the analysed range of the depth of cut the components of the resultant force increase with increasing depth of cut. Ra, Rz and Rvk decrease with increasing depth of cut, which can be explained by the less proportion of pulled out coating material and opened pores. The analyses of Vvv confirm this. The residual stresses decrease in the feed direction and increase in the cutting direction with increasing depth of cut.

The relations shown increase the knowledge in machining of thermally sprayed coatings by tools with geometrically defined cutting edges. This represents an essential step for the substitution of the common honing process in finish machining of thermally sprayed coatings.

## References

- [1] Bobzin K, Ernst F, Richardt, K, Schlaefler T, Verpoort C and Flores G 2008 Thermal spraying of cylinder bores with the Plasma Transferred Wire Arc process *Surf. Coat. Tech.* **268** 4438-4443
- [2] Hoffmeister H W and Schell C 2008 Mechanical roughing of cylinder bores in light metal crankcases *Prod. Engineer* **2** 365-370
- [3] Liborius H, Paczkowski P, Nestler A, Grund T, Schubert A and Lampke T 2018 Influence of dovetail microstructures on adhesive tensile strength and morphology of thermally sprayed metal coatings *Proc CIRP* **71** 299-304
- [4] Ding K and Sasahara H 2012 Thermal Spray Coating for Sleeveless Engine Cylinder *Adv. Mat. Res.* **472-475** 991-996
- [5] Liborius H, Paczkowski P, Nestler A, Grund T, Mehner T, Schubert A and Lampke T 2019 Influence of cutting speed on the surface properties in turning of Fe17Cr2Ni0.2C iron based thermally sprayed coatings *International Conference on Competitive Manufacturing (COMA 19) Proceedings* 63-67